Since January 2020 Elsevier has created a COVID-19 resource centre with free information in English and Mandarin on the novel coronavirus COVID-19. The COVID-19 resource centre is hosted on Elsevier Connect, the company's public news and information website.

Sustainable Cities and Society 77 (2022) 103548

Contents lists available at ScienceDirect

Sustainable Cities and Society

journal homepage: www.elsevier.com/locate/scs

Airflow deflectors of external windowsto induce ventilation: Towards COVID-19 prevention and control

Wanqiao Che [a,1], Junwei Ding [b,1], Liang Li [a,*]

[a] School of Design, Central Academy of Fine Arts, Beijing, China
[b] School of Architecture, Southeast University, 2 Sipailou, Nanjing, Jiangsu, China

ARTICLE INFO

Keywords:
Natural ventilation
Airflow deflectors
Air diffusion performance
Transmission rate
Low-cost renovation

ABSTRACT

Since the Corona Virus Disease 2019 (COVID-19) outbreak, the normalization of the epidemic has posed great challenge to epidemic prevention and control in indoor environment. Ventilation systems are commonly used to prevent and control indoor transmission of disease. However, most naturally ventilated rooms are not efficient to prevent the spread of virus, i.e., classrooms. The goal of this work is to effectively adopt forced interference strategies (e.g., airflow deflector) applied to external windows to strengthen airflow diffusion performance (ADP) of natural ventilation. So far, no systematic study has been done to investigate the effectiveness of such airflow deflectors on its influence on natural ventilation and effectiveness of preventing the disease transmission in indoor environment. In this work, a case study was conducted based on cross-ventilated classrooms. Different settings of airflow deflectors (i.e., size and installation angle) were applied to the external windows. Air Diffusion Performance Index (ADPI) was utilized to evaluated airflow diffusion performance under different settings of the airflow deflectors. Then, the Wells-Riley model was applied to evaluate infection risk. According to the results, the infection risk can be reduced by 19.29% when infection source is located at the center of classroom and 17.47% when source is located near the side walls. This work would provide guidance for the design of classrooms ventilated with induced natural wind for epidemic prevention and control.

1. Introduction

The outbreak of pneumonia caused by Corona Virus Disease 2019 (COVID-19) raises serious social concern. Up to 17 October 2021 (17:00 GMT), more than 200 countries, areas or territories have been reporting infection cases of COVID-19 (COVID-19); Feng, Cao, Wang, Kumar, & Haghighat, 2021), which indicates the severity of the world-wide pandemic. The rapid transmission of COVID-19 has had a big impact on the social activities with respect to all sides of the city including transportation, production and life of citizens (Cai et al., 2021; Wu et al., 2021). The recent report of COVID-19 in Putian, Fujian province of China, declared the hidden transmission for at least 10 days in primary schools (China, 2021), resulting the infection of 19 students in six schools. Once the epidemic prevails among students, it would pose huge challenge to epidemic prevention and control. As a place where students stay for a long time and study, classrooms have also become potential sites for the spread of the disease. Therefore, attention should be paid to the prevention and control of the epidemic in naturally ventilated classrooms.

Generally, the transmission of COVID-19 consists of two main routes (Ding, Yu, & Cao, 2020; Xu, Luo, Yu, & Cao, 2020), namely contact transmission and droplet transmission. As to droplet transmission, smaller virus-containing droplets and particles (known as aerosols with the diameter less than 5 μm) can be suspended in the air over long distances (Ding et al., 2020). In this context, Centers for Disease Control and Prevention (CDC) and REHVA are calling for considerable attention (Improving Ventilation in Your Home, 2021) to airborne transmission of COVID-19 through improvement to indoor air quality in public buildings, such as purification of indoor air (Zhu, Ren, & Cao, 2021), increase in outdoor air supply, avoidance for recirculated polluted air (Sha, Zhang, & Qi, 2021), etc. On the one hand, these improvement manners reply on mechanical ventilation systems (Wang, Huang, Feng, Cao, & Haghighat, 2021), which is not feasible for architectures ventilated with naturally induced wind (e.g., classrooms with high-densified occupants). Especially for the protection of vulnerable groups (Zivelonghi & Lai, 2021), these suggestions and manners applied to mechanical

* Corresponding email at: China Central Academy of Fine Arts, Beijing, China.
E-mail address: zmliang@126.com (L. Li).
[1] Equal contribution.

https://doi.org/10.1016/j.scs.2021.103548
Received 21 October 2021; Received in revised form 11 November 2021; Accepted 14 November 2021
Available online 18 November 2021

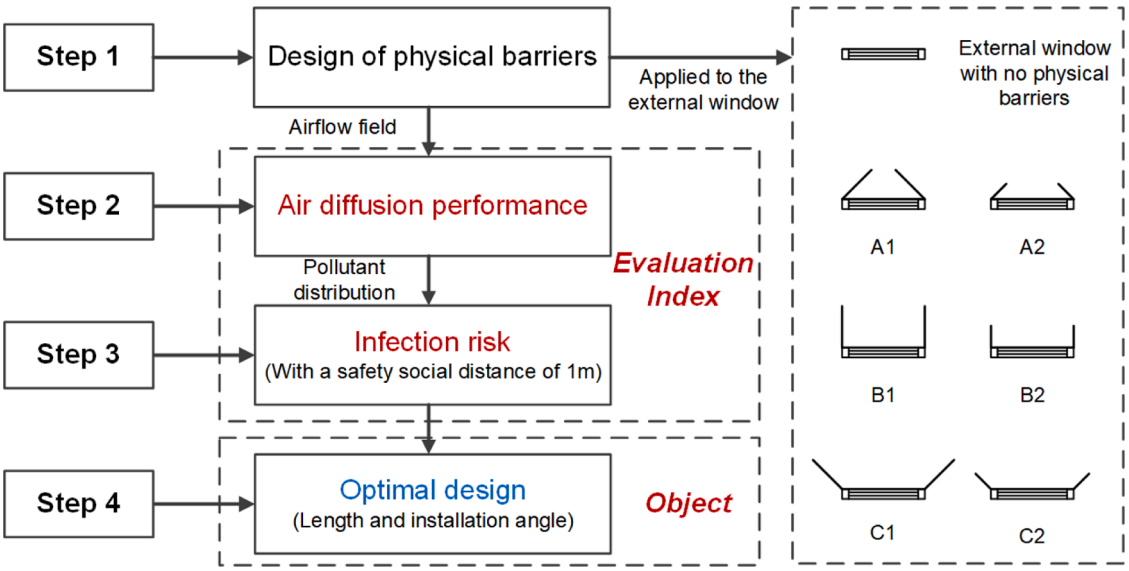

Fig. 1. Flowchart of this work aimed at the optimal design of airflow deflectors for a safe indoor environment ventilated by induced wind through external windows.

ventilation systems can do little favor. On the other hand, mechanical ventilation systems may consume large amount of energy consumption (Cao, Dai, & Liu, 2016; Li, Shen, & Yu, 2017), which is not beneficial for the sustainable development of society. Thus, it is necessary to do research on the design of natural ventilation systems under the situation of epidemic prevention and control (Corticos & Duarte, 2021; Park, Choi, Song, & Kim, 2021). Natural ventilation is a kind of passive green building technology using thermal pressure caused by the density difference of air inside and outside the building or the wind pressure caused by outdoor atmospheric movement to induce outdoor fresh air (Gautam, Rong, Zhang, & Abkar, 2019; Moey, Chan, Tai, Go, & Chong, 2021). As an environment-friendly and energy-saving method, natural ventilation is becoming one favorable option to potentially improve the indoor air quality (Bayoumi, 2021) and lower the risk of disease exposure (M.Gil-Baeza, Villanuevacd, M.Molina-Huelvaab, & Chacarteguicd, 2021). It is demonstrated that natural ventilation can reduce indoor air pollutants originating from outdoor sources in the range of 5%-20% (Chen, Gall, & Chang, 2016). Through investigating the significant effect of natural ventilation paths on the pollutant dispersion and airflow characteristic, the maximum reduction of 50% in pollutant concentration for a cross-ventilated building was quantified by Liu et al. (Liu, Lv, Peng, & Shi, 2020).

However, the performance of natural ventilation is limited to multiple internal and external factors (building structure, prevailing wind direction, climatic conditions) (van Moeseke, Gratia, Reiter, & De Herde, 2005), which makes the analysis of cross-ventilation in buildings quite complex (e.g., the method of tracer gas (Nikolopoulos, Nikolopoulos, Larsen, & Nikas, 2012) is commonly used in the analysis of cross-ventilation). In addition, the fast transmission of COVID-19 pandemic has indicated that the current cross-ventilation design schemes (e.g., design of doors and windows (Chen, Feng, & Cao, 2020)) of most buildings may be insufficient to provide the required ventilation rate to avoid the transmission of infectious diseases (Guo et al., 2021). Especially in public buildings and spaces (e.g., schools, libraries, offices, etc.), the ventilation levels based on the current cross-ventilated systems (Zheng, Ortner, Lim, & Zhi, 2021) are apparently lower than the recommended ventilation standards towards COVID-19. For instance, it is strongly suggested that the ventilation rate should be 2 (h^{-1}) with a mask and 7 (h^{-1}) without a mask when staying in a classroom for above 2 hours (Rothamer, Sanders, Reindl, & Bertram, 2021). Therefore, optimizing the design of cross-ventilated through low-cost renovation is worth investigating and can provide good assist in spread control of COVID-19. Airflow deflector is a kind of low-cost renovation method to improve airflow diffusion (Ren et al., 2021). The work theory of airflow deflector mainly depends on the pressure difference created by physical constructions to induce the direction change of airflow . There are limited literature and case studies on the validation of external deflector strategies (e.g., airflow deflector) to enhance the air diffusion performance of natural ventilation. To fill this gap, a typical wind-driven naturally ventilated classroom (on the third floor) is chosen as the target object in the present study to optimize the air diffusion of window opening natural ventilation rooms.

In this work, we first analyzed the limitations of ventilation in high-rise buildings through the numerical simulation results of airflow distribution. Then, the existing natural ventilation mode is optimized through low-cost renovation (installation of airflow deflectors to external windows). On this basis, the airflow and pollutant concentration distributions under different installation of airflow deflectors were compared and the overall performance is evaluated. In order to obtain the optimal combined ones, the indicators of ventilation efficiency (ADPI value) and infection risk (IR value) were utilized. This work can be referred to by designers for improving the efficiency of natural ventilation and disease control in classrooms as well as other alike public buildings.

2. Methodology

The flowchart of this work is shown in Fig. 1. First, the airflow deflectors are designed to improve the air diffusion of natural ventilation classroom. Then the air flow field was simulated through the computational fluid dynamic method based on the indoor and outdoor combined boundary. The infection risks are evaluated on the hypothesis of a safe social distance in the classroom (i.e., at least 1 m). Finally, based on the normal opening mode of four external windows, the length and installation angle of airflow deflectors are determined for the optimal design by considering ventilation efficiency and infection probability.

2.1. The model of classroom

The target object of this research is a wind-driven naturally ventilated classroom, which is located on the 3rd floor of a university building, as displayed in Fig. 2 **(a)**. The size of the classroom is 14.0 m (X) × 8.5 m (Y) × 5.0 m (Z) with a total volume of 595 m^3. There are 2 doors and 6 windows (with a maximum opening of 4 windows) used for

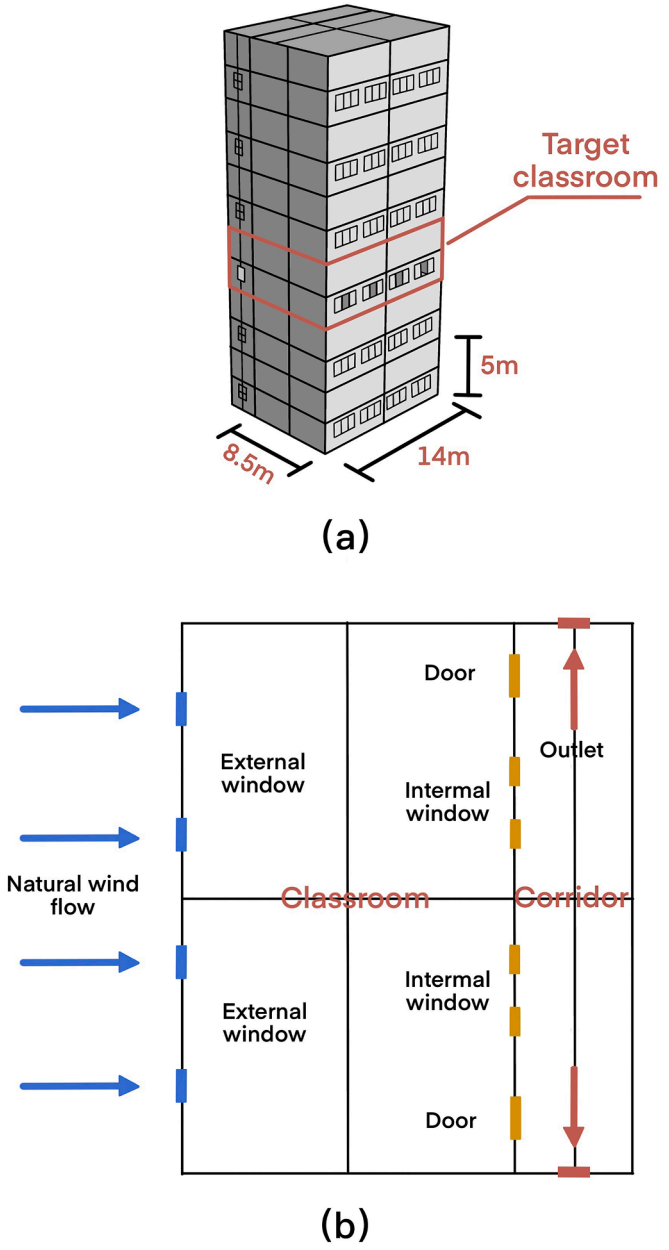

Fig. 2. (a)The model of the classroom applied in this research (b) The layout of the target classroom on the third floor (the coordinate of source A is (0, 0) at the center of the classroom, and the coordinate of source B is (0, 5), 2 m away from the side walls).

ventilation on the corridor side of the classroom (ref. Fig. 2 **(b)**), 12 push-pull windows (with a maximum opening of 4 windows) for ventilation and 8 sealed south windows for lighting on the exterior wall side (ref. Fig. 2 **(a)**). The classroom mainly obtains cross-ventilation by natural wind flow induced from the opening external window. Then the wind flow crosses the doors and windows on the inner wall to the corridor and emits to the outdoor through the external window (outlet) (ref. Fig. 2 **(a)**). The dimension of each window on the external wall is 0.8 m (X) × 1.1 m (Z) and the dimension of each window on the inner wall is 0.8 m (X) × 0.7 m (Z). The door size is assumed as 1.1 m (X) × 2.1 m (Z).

2.2. Simulation setups and grid independence analysis

The commercial software of ANSYS FLUENT 18.0 is adopted for the numerical simulations in this study.

An incompressible and steady-state Reynolds-averaged Navier-Stokes (RANS) model and the *Re*-Normalization Group (RNG) k-ε model was adopted (van Hooff, Blocken, & Tominaga, 2017) as RANS turbulence model for better simulation of indoor environmental parameters (Shirzadi, Tominaga, & Mirzaei, 2020; van Hooff & Blocken, 2020), such as airflow velocity, pollutant concentration, etc.

The general form of the governing equation can be written as:

$$\nabla\cdot(\rho\mathbf{u}_i\phi) - \nabla\cdot(\Gamma\nabla\phi) = S \quad (1)$$

ρ is the density; $\mathbf{u}_i$ is the velocity vector; ϕ represents each of three velocity components, kinetic energy of turbulence, dissipation rate of kinetic energy of turbulence, air temperature and pollutant concentration; Γ is the effective diffusion coefficient; and S is the source term of the equation.

2.2.1. Computational domain

Since the simulation about natural ventilation is generally carried out on the basis of the computational domain using outdoor boundary, it would require large computational intensity without simplification of the simulation geometry by using indoor boundary (e.g., the average velocity or pressure of the window openings based on the computational domain using outdoor boundary is employed as indoor inlet boundary condition). However, considering the function of airflow deflectors on inducing outdoor air, we still apply computational domain using outdoor domain, as shown in **Fig.** 3 (a). A rectangular domain was created for the CFD simulations. The mesh was constructed using ICEM CFD and the total number of grids reached 14 million. Moreover, the tetrahedral meshes around the target building was densified by exponential function method. The tetra size ratio was set as 1.1 to make the transition from small meshes to large meshes.

2.2.2. Boundary conditions of outdoor domain

For outdoor domain in Fig. 3 (b), the rectangle domain was created in accordance with the most common practice guidelines for the CFD simulation (Tominaga et al., 2008; van Hooff et al., 2017). The inlet is at a 5H distance upstream and the outlet is at a 10H distance downstream (with the height H of 30 m). The lateral and top boundaries are at 5H distances away from the targeted building. Table 1 indicates the boundary conditions assigned to the computational domains using outdoor boundary. The gradient wind was applied to the inlet boundary of computational domain to simulate natural air flow under the influence of atmospheric boundary layer (Meng, Cao, Kumar, Tang, & Feng, 2021; Xi, Ren, Wang, Feng, & Cao, 2021). The inflow profile of wind speed (U_z) follows the power-law type wind model with a power-law exponent (α) of 0.3, and reference wind speed (U_{ref}) is taken as 2.62 m/s at a reference height (H_{ref}) of 10 m (i.e., the measured average wind speed). In order to validate the effectiveness of airflow deflector under extreme conditions, the direction of wind and building was set as 0 °. Under this circumstance, we mainly focus on the relationship between airflow reflectors and infection rates. The outlet is associated with the outflow boundary condition, and the top and lateral boundaries are modeled with symmetry boundary condition. The geometric roughness height for the ground is 1.3 m with a roughness height constant of 7.

2.2.3. Boundary conditions of indoor domain

As regards the boundary conditions of classroom, all classroom surfaces are configured as non-slip walls. Four windows (ref. Fig. 2, the opening windows denoted by blue blocks) are opened in the classroom, which can be indicated as the normal window opening mode. That is to say, the installation of airflow deflectors is based on the normal opening mode of windows.

According to World Health Organization (WHO), viruses such as COVID-19 mainly spread by means of droplets and aerosols when an infected person coughs or sneezes. Droplets will fall to the ground or

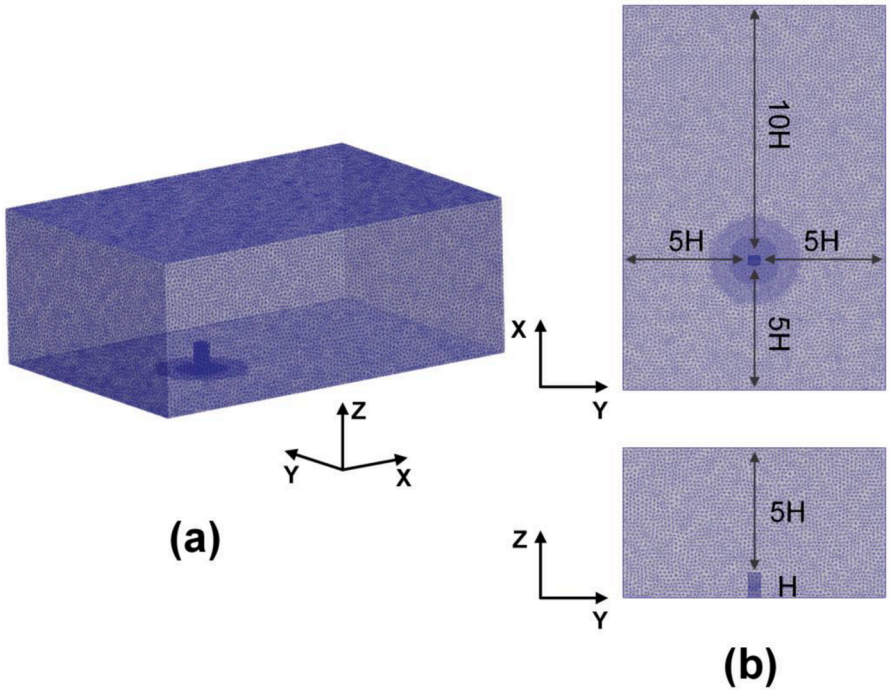

Fig. 3. (a) Example of the simulation mesh used; (b) The size of computational domain (H=30 m).

Table 1
The type of outdoor boundary and corresponding boundary conditions of the computational domain.

Boundary	Type	Conditions
Inlet	velocity-inlet	$U_z = U_{ref} \cdot (z/H_{ref})^{\alpha}$ (Xi et al., 2021)
Outlet	outflow	
Ground	rough wall	roughness height of 1.3 m with a roughness height constant of 7
Top and laterals	symmetry	
Classroom	wall	non-slip wall

Table 2
The specification of designed deflectors.

No. Airflow deflectors	Installation angle degree	Length of Airflow deflectors
N	NONE	NONE
A1	45 degrees	D/2
A2	45 degrees	D/4
B1	90 degrees	D/2
B2	90 degrees	D/4
C1	135 degrees	D/2
C2	135 degrees	D/4

Note: D is the width of each window for ventilation (D = 0.8 m).

Table 3
The infection risk with pollutant source of location A and B.

	Infection risks	
	Source location A	Source location B
N (No Deflectors)	41.05%	57.47%
A1 (45°, D/2)	38.73%	42.04%
A2 (45°, D/4)	40.26%	40.00%
B1 (90°, D/2)	21.76%	47.22%
B2 (90°, D/4)	24.05%	46.46%
C1 (135°, D/2)	36.85%	52.35%
C2 (135°, D/4)	40.26%	48.81%

Note: The exposure time of occupants to the indoor environment is 1 hour.

surfaces with the distance less than 1 m, while aerosols behave like gas through spreading to longer distances before settling on the surfaces. Due to the safe social distance of at least 1 m between the occupants should be guaranteed under the normalized control of COVID-19, we mainly focus on infection risks caused by long distance transmission (Pei, Taylor, & Rim, 2021). Thus, simulations of pollutant concentration were conducted to the evaluate the infection risk caused by an infected occupant, which is associated with the flow turbulence. From the study by Leng et al. (Leng, Wang, & Liu, 2020), the pollutant source intensity of an infected occupant can be assumed as 1E-04 (quantum/m^3), which is further used as a reference value for pollutant concentration (C_{ref}) in this work. The pollutant sources in this study are assumed as the COVID-19 infected occupants, who may generate virus-carrying droplets or aerosols by coughing. According to the work of Chen et al. (Chen et al., 2014), it is reasonable to simulate exhaled droplets as gaseous pollutants. Here, we applied two gaseous pollutants on the basis of flow filed with different window deflectors. The location of selected sources is shown in Fig. 2 (b). Source A is located at the center of the classroom and source b is located 2 m away from the side wall.

2.3. Design of airflow deflectors

Following the three steps in the above-mentioned flowchart of Fig. 1, the next study design starts with the installation of airflow deflectors in the targeted classroom, (i.e., size of airflow defectors and installation angle). The current window opening is renovated from the perceptive of enhancing the air diffusion performance due to the insufficient fresh air volume, which is realized by different specification of airflow deflectors as shown in Table 2. As to the installation angle of airflow deflector, we divide 0 ° to 180 ° equally into four intervals (0 °, 45 °, 90 °,135 ° and 180 °) and select the median as installation angle, i.e., 45 °, 90 ° and 135 °. In order to ensure that the airflow deflector can rotate freely through 0 ° to 180 °, the length of the airflow deflector is designed full length and half length of the window frame. The installation of the window-integrated deflectors is further considered to potentially reduce the infection risk. The evaluation models used for ***current opening mode, renovated window openings with installed airflow deflectors*** are

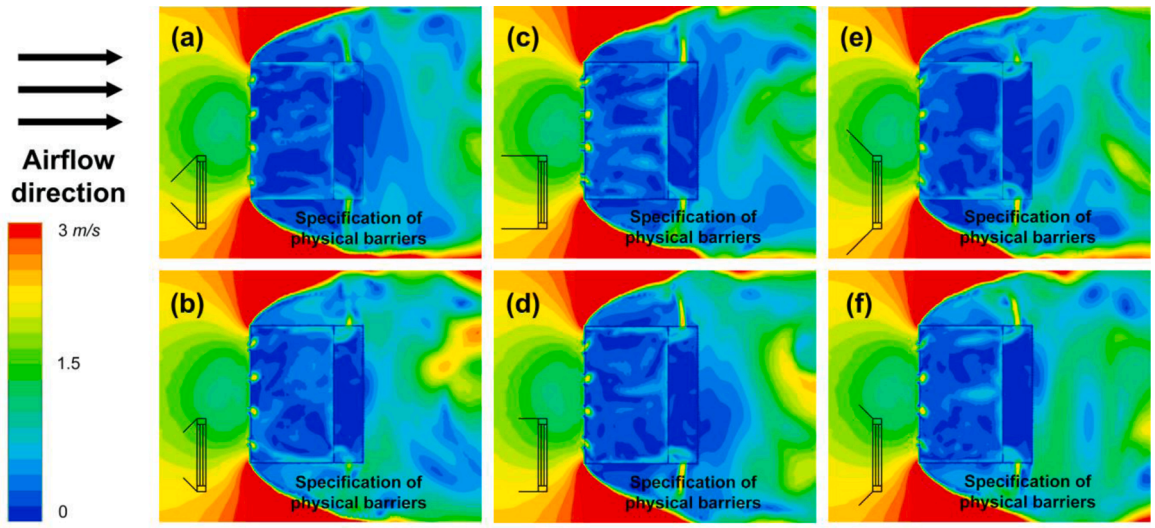

Fig. 4. The simulation results of indoor airflow field with different airflow deflectors installed under the opening mode of four windows (a) airflow deflector of A1, (b) airflow deflector of A2, (c) airflow deflector of B1, (d) airflow deflector of B2, (e) airflow deflector of C1 and (f) airflow deflector of C1. The height of the x-y plane is 11.2 m, equaling to 1.2 m upon the third floor.

discussed in the Section 2.4.

2.4. Models for performance evaluation

In this section, two evaluation models are applied to investigate the function of airflow deflectors on the airflow distribution and its performance on the control of disease infection induced by long distance transmission, respectively are air diffusion performance index and infection risks. The calculation methods of ADPI index and infection risks are as below.

2.4.1. Air diffusion performance index

In this work, an Air Diffusion Performance Index (ADPI) model is utilized to evaluate the airflow distribution performance under seven conditions of renovated window opening with installed airflow deflectors (ref. Table 2). ADPI is defined as the percentage of occupant zone (e.g., a height of 1.2 m upon the floor) falling into the acceptable indoor velocity and temperature region determined by measuring local Effective Draft Temperature (EDT), as shown below(ANSI/ASHRAE, 2009).

$$ADPI = \frac{\sum_{j=1}^{M}(P_E)_j}{\sum_{i=1}^{N}P_i} \times 100\% \tag{2}$$

Where, P_i is the measuring point in the occupied area (i = 1, 2, …N, and N is the total number of P_i); and P_E represents the measuring point falling into the acceptable velocity and temperature region by calculating the EDT value (j = 1, 2, …M, and M is the number of P_E). The EDT (°C) can be written as follows.

$$EDT(i) = (t_i - t_a) - 8.0(v_i - 0.15) \tag{3}$$

where, t_i (°C) is air temperature at the measuring point of i; t_a (°C) is average air temperature in the occupied region; and v_i (m/s) is local air velocity. Since the temperature factor is not considered in this study, the value of $(t_i - t_a)$ in Eq. (3) can be assumed to be zero, i.e., the temperature distribution approximately achieves uniformity. Then, Eq. (3) can be rewritten as follows.

$$EDT(i) = -8.0(v_i - 0.15) \tag{4}$$

The criterion range of EDT is between −1.7 °C and 1.1 °C with the velocity less than or equal to 0.35 m/s. With the lower limit of EDT (−1.7 °C), 80% of the occupants can feel comfortable (Liu & Novoselac, 2015). Therefore, the ventilation performance is generally accepted when ADPI value is greater than 80%.

2.4.2. Infection risk

In order to investigate the infection risk for occupants at the circumstance of different specifications of airflow deflector and pollutant sources, an evaluation model based on the Wells-Riley equation (Riley, Riley, & Murphy, 1978; Rudnick & Milton, 2003) is applied for infection risk investigation in this study, which is expressed as below:

$$R = \left(1 - exp\left(-IR * \int_0^T C(t)dt\right)\right) * 100\% \tag{5}$$

where, R represents the infection risk (%); t is the time (h); T is the total exposure time (h); $C(t)$ represents the pollutant concentration (quantum/m^3); IR is the inhalation rate of exposed occupant (m^3/h). In this research, the IR value is defined as 0.96 (m^3/h) (Buonanno, Stabile, & Morawska, 2020) for indoor active occupants, and the total exposure time is set as 1 hour for favorable assessment of infection risk.

3. Results

In this section, the numerical simulation results are processed for further research. On the premise of numerical simulation results and the models (air diffusion performance and infection risk) in Section 2.4, indoor ventilation performance and probability of disease infection are analyzed under different specifications of airflow deflectors as well as infected sources in a cross-ventilated classroom. Firstly, the results of airflow field in the natural ventilation classroom equipped with 6 different airflow deflectors (ref. Table 2) are shown. In order to compare the air diffusion performance, the corresponding values of ADPI is plotted. The infection risk of each case is obtained and compared for the optimal mode for airflow deflectors.

3.1. Results of airflow distribution and air diffusion performance

On the basis of the different specifications of airflow deflectors installed under the window opening mode of four windows, the airflow distribution performance is analyzed by directly using computational domain in combination of outdoor and indoor boundary conditions. Fig. 4 illustrates the contour of velocity field at the plane of z = 11.2 m (equaling to 1.2 m upon the third floor), respectively are the six

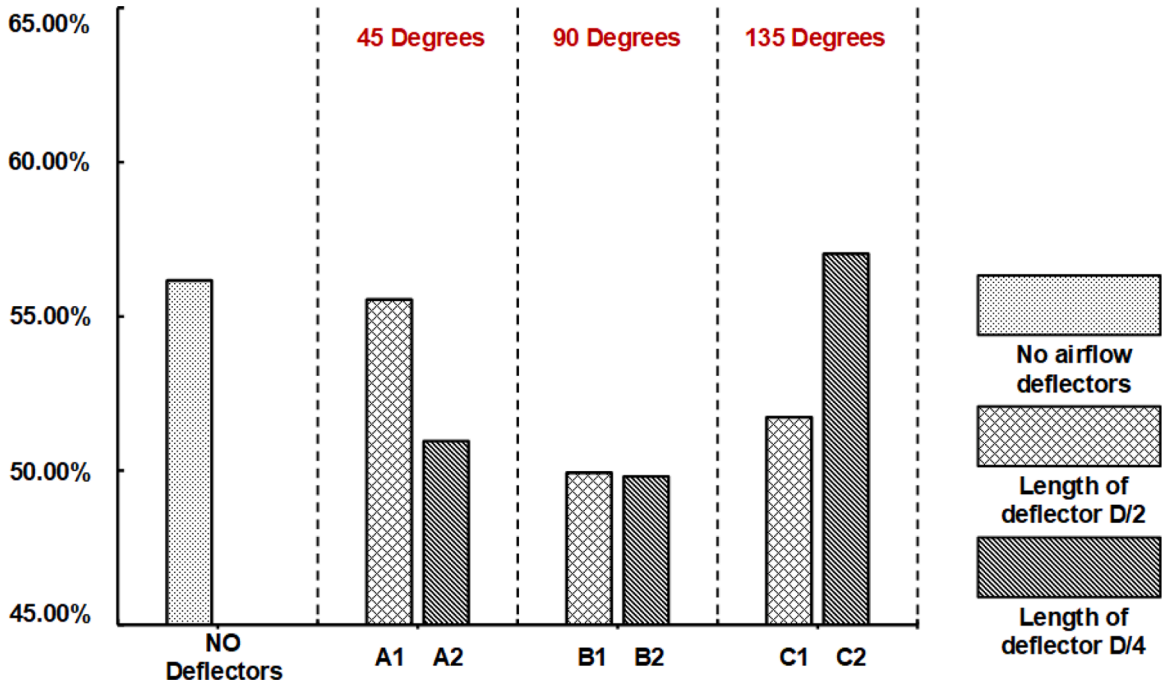

Fig. 5. Ventilation index (ADPI values) between different speification of airflow deflectors (a) airflow deflector of A1, (b) airflow deflector of A2, (c) airflow deflector of B1, (d) airflow deflector of B2, (e) airflow deflector of C1 and (f) airflow deflector of C1.

renovated window opening with reflectors of A1, A2, B1, B2, C1 and C2. There is a significant increase of high velocity area at a height of 1.2 m (i.e., breathing zone of occupants) as the airflow deflectors play the role of introducing outdoor air into the classroom. Among these modes, modes B1, B2, C1 and C2 all provide large coverage area of supply air. For modes A1 and A2, the intensity of airflow is weaker in the respiratory area and the distribution of velocity magnitude at the height of z=1.2 m is more uniform, compared with the modes of B1, B2, C1 and C2.

In order to further quantify the ventilation performance, Fig. 5 indicates the ADPI values for the original mode with no deflectors and renovated window opening with reflectors of A1, A2, B1, B2, C1 and C2, respectively. It can be seen that the ADPI values for window opening with reflectors of B1 and B2 are significantly decreased compared to the original mode with no deflectors of 56.2%. The ADPI values for modes B1 and B2 are respectively about 49.9% and 49.8%. It can be seen that when the installation angle of airflow deflectors is set as 90 °, the ADPI value of different lengths of deflectors shows little difference. For the modes of A1, the ADPI is 55.5% and approximately equals to the original mode with no deflectors, indicating that the effect of this renewed mode is negligible on improving the airflow distribution performance. For the specification of C2, the ADPI 57.0% is a little higher than the original mode.

However, as described in subSection 2.4.1, the ventilation performance can be satisfactory when the ADPI is equal to 80% at least. Thus, it can be summarized that all the natural ventilation modes with or without airflow deflectors are insufficient to ensure a comfortable indoor environment for cross-ventilated classroom from the perspective of airflow pattern. Due to the function of airflow deflectors on introducing outdoor air, there is no marked improvement to the ADPI for occupants' comfort (an ideal air flow velocity of 0–0.35 m/s). However, for the sake of delivering more fresh air to the classroom, the ADPI value for comfort cannot be the only judgement. In addition, the infection risk is another

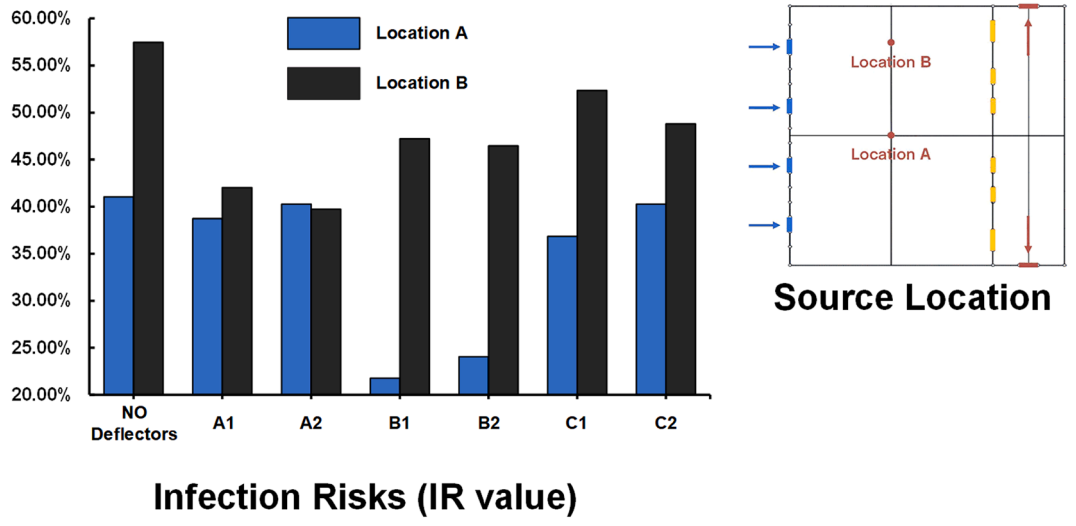

Fig. 6. Percemtage of infection risks (IR values) between different specification of airflow deflectors with pollutant source at location A and B.

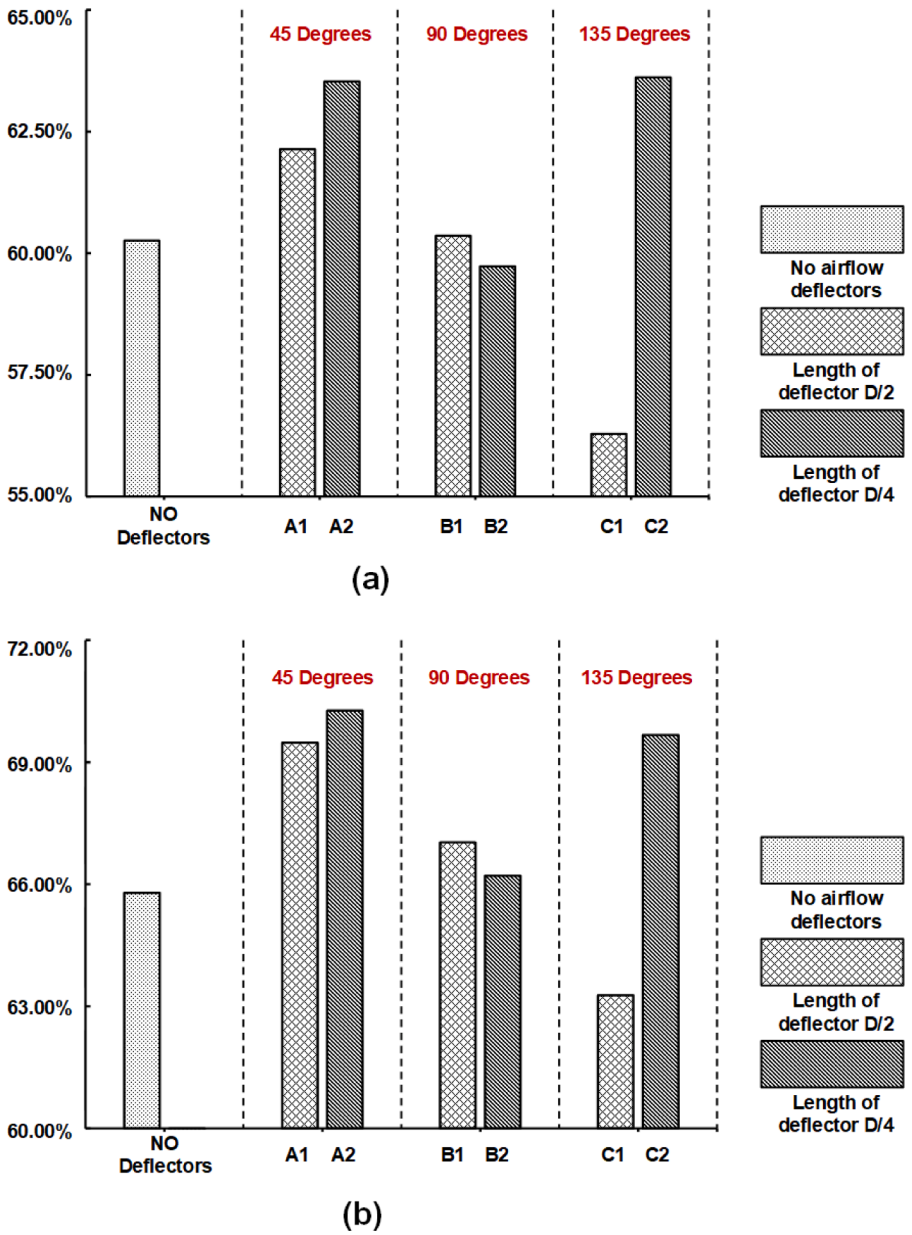

Fig. 7. The ventilation index (ADPI values) (a) under the EDT scope of 0–0.5 m/s (b) under the EDT scope of 0–0.6 m/s.

point to consider when it comes to the function of airflow deflectors on the creation of a comfortable and safe indoor environment. Therefore, in the next section, we compared the average infection risks of all the seven window openings equipped with different airflow deflectors when pollutant source is located at two different locations.

3.2. Influence of air flow deflectors on airflow distribution and infection risk

By utilizing the infection risk assessment model, the infection probabilities under a variety of window openings equipped with different airflow deflectors and two pre-set locations of pollutant source are calculated. Regarding the single source of A at the center of the classroom and the single source B near the side wall, the average infection risk around the occupied zones under 1.2 m is obtained. Fig. 6 depicts the infection likelihood (1 hour of exposure to the environment of target classroom is set for calculation) under pollutant sources of A and B between the opening of windows with no airflow deflectors and the ones equipped with different specification deflectors of A1, A2, B1, B2, C1 and C2.

When the source is released at location A, the infection risk of the original opening with no deflectors is 41.05%. With respect to modes B1 and B2, the calculated infection probability of occupants shows a large decrease compared with the original mode. However, the renewed modes A1, A2, C1 and C2 play negligible roles in mitigating the transmission of infectious diseases. Besides, it can be noted that when the source is located at B, the corresponding infection risks are commonly higher than that of location A. The reason is analyzed as the location of source A is closer to the window inlet with more significant influence of the jet zone (straightly from inlet to outlet) (Cao, Ding, & Ren, 2020; Ding & Cao, 2021), which can facilitate the discharge of more pollutants to the outlet. As the distance between the source location and the inlet increases, the effect of the jet diminishes. Under the impact of backflow and turbulence, there is a tendency for pollutant to spread around, which further results in an increase in global concentration and infection risk. It is notable that all the renovated ones with airflow reflectors have at least a 5.12% reduction in the infection risks when the source is located at position B.

In general, the ADPI values fail to reach the expected target of 80% for the original window opening with no deflectors as well as all renovated modes with deflectors. Nevertheless, the renovated window opening with reflector A1 and C2 can exhibit favorable performance in the improvement of airflow distribution and reduction of infection risk compared to the window opening with no deflectors when the source is at location B. However, when the source is at location A, mode B1 is selected as the optimal one during all the designed airflow deflectors in this study, taking the transmission possibility as the priority.

4. Discussion

It is of great significance to acquire a safe and comfortable indoor environment in naturally ventilated classrooms through some low-cost prevention measures during outbreak of COVID-19. This study focuses on optimizing the airflow deflectors installed to the external window based on the opening mode (4 windows opened) of a typical cross-ventilated classroom to effectively mitigate the propagation of indoor infectious diseases.

According to the results in Section 3, the original window opening with no airflow deflectors shows a relatively high infection risk averagely in the respiratory zone of the target classroom. As is mentioned in Section 2.4.1, EDT values for a natural ventilation system is defined as 0 m/s to 0.35 m/s in order to guarantee the satisfaction of 80% indoor occupants. Under this condition, although the air diffusion performance of target classroom equipped with airflow deflectors is no significantly improved or even worse than the original window opening with no airflow deflectors. When it comes to the design of cross-ventilated classroom under the situation of epidemic control, the standard of infection risk should be the priority. Thus, we compared the ventilation index of ADPI when we enlarge the acceptable scope of EDT value from 0–0.35 m/s to 0–0.5 m/s and 0–0.6 m/s. Fig. 7 displays the ADPI values for the original mode with no deflectors and renovated window openings with reflectors of A1, A2, B1, B2, C1 and C2, respectively. Fig. 7 **(a)** represents the ADPI values under the EDT scope of 0–0.5 m/s and Fig. 7 **(b)** represents the ADPI values under the EDT scope of 0–0.6 m/s. Compared with the ADPI values in Fig. 5 using the EDT scope of 0–0.35 m/s, the ADPI is significantly improved in mode A1 by 12%, in mode C1 by 13.5% and in mode C2 by 13.3%. The mode C2 shows a good performance on all the ADPI value and infection risk under. Thus, appropriately increasing the standard of wind speed can reduce the risk of infection.

The limitations of this work are described below. In the simulation of pollutant concentration field, the gas contaminant is mainly considered instead of using tracer mass and particle matter. The short-distance transmission risks caused by the evaporation of liquid droplets (from large particles to small ones) is negligible in this work. Instead, we only investigated the long-distance transmission on the premise of a safety social distance of at least 1 meter. For a real environment in the classroom, more detailed set up of numerical simulation (including models, boundary conditions, etc.) should be paid attention to for effective practical application. As regards more poorly designed and ventilated classroom, the possible combinations of low-cost and convenient tools need to be validated for lower infection risk and broader application prospect, e.g., air purification (Chen et al., 2021), exhaust fan (Wu & Niu, 2016), ultraviolet germicidal irradiation (UVGI) (Feng, Cao, & Haghighat, 2021; Su, Lau, & Gibbs, 2016), etc.

5. Conclusions

This work investigates the impact of the design of airflow deflectors installed to the external window on airflow distribution performance and infection risk in a wind-driven natural ventilated classroom through using the simulation method based on the combination of indoor and outdoor boundary. On account of the window opening mode of four external windows, a series specifications of airflow deflector are designed and the performance is compared in order to acquire an optimal one. By installing the airflow deflectors at the external window, the ventilation efficiency is enhanced with the risk of disease transmission reduced. This study can provide a reference for the design and renovation of typical cross-ventilated classrooms during the epidemic normalization phase. The main findings are shown as follows.

(1) The original window opening with no airflow deflectors and six renovated ones with different specification of airflow deflectors all fail to reach the targeted requirement of 80% for ADPI. Among them, the mode A1 (45 ° and 1/2 length) and C2 (135 ° and 1/4 length) are regarded as the ones with the acceptable ADPI value.
(2) The infection risk is lower when the location of source is closer to the window inlet with more significant influence of the jet zone (straightly from inlet to outlet), which can facilitate the discharge of more pollutants to the outlet.
(3) When pollutant source was set at position A, the mode B1 (90 ° and 1/2 length) has the best performance on reducing the infection risk by 19.29%. When pollutant source was set at position B, the mode A2 (45 ° and 1/4 length) has the best performance on reducing the infection risk by 17.47%.

Declaration of Competing Interest

The authors declare that this paper has no conflict of interests. Paper has not been submitted or published elsewhere.

References

ANSI/ASHRAE. (2009). Method of testing for room air diffusion. *ANSI/ASHRAE standard* (pp. 113–2009). Atlanta: American Society of Heating, Refrigerating and Air-Conditioning Engineers, Inc..

Bayoumi, M. (2021). Improving indoor air quality in classrooms via wind-induced natural ventilation. *Modelling and Simulation in Engineering*, 2021. https://doi.org/10.1155/2021/6668031

Buonanno, G., Stabile, L., & Morawska, L. (2020). Estimation of airborne viral emission: Quanta emission rate of SARS-CoV-2 for infection risk assessment. *Environment International*, 141. https://doi.org/10.1016/j.envint.2020.105794

Cai, W. J., Wang, H. W., Wu, C. L., Lu, K. F., Peng, Z. R., & He, H. D. (2021). Characterizing the interruption-recovery patterns of urban air pollution under the COVID-19 lockdown in China. *Building and Environment, 205*, Article 108231. https://doi.org/10.1016/j.buildenv.2021.108231

Cao, S. J., Ding, J. W., & Ren, C. (2020). Sensor deployment strategy using cluster analysis of Fuzzy C-Means Algorithm: Towards online control of indoor environment's safety and health. *Sustainable cities and society* (p. 59). https://doi.org/10.1016/j.scs.2020.102190

Cao, X. D., Dai, X. L., & Liu, J. J. (2016). Building energy-consumption status worldwide and the state-of-the-art technologies for zero-energy buildings during the past decade. *Energy And Buildings, 128*, 198–213. https://doi.org/10.1016/j.enbuild.2016.06.089

Chen, A. L., Gall, E. T., & Chang, V. W. C. (2016). Indoor and outdoor particulate matter in primary school classrooms with fan-assisted natural ventilation in Singapore. *Environmental Science and Pollution Research, 23*(17), 17613–17624. https://doi.org/10.1007/s11356-016-6826-7

Chen, C., Zhu, J. C., Qu, Z. J., Lin, C. H., Jiang, Z., & Chen, Q. Y. (2014). Systematic study of person-to-person contaminant transport in mechanically ventilated spaces (RP-1458). *Hvac&R Research, 20*(1), 80–91. https://doi.org/10.1080/10789669.2013.834778

Chen, T. S., Cao, S. J., Wang, J. Q., Nizamani, A. G., Feng, Z. B., & Kumar, P. (2021). Influences of the optimized air curtain at subway entrance to reduce the ingress of outdoor airborne particles. *Energy and Buildings*, 244. https://doi.org/10.1016/j.enbuild.2021.111028

Chen, T. S., Feng, Z. B., & Cao, S. J. (2020). The effect of vent inlet aspect ratio and its location on ventilation efficiency. *Indoor and Built Environment, 29*(2), 180–195. https://doi.org/10.1177/1420326x19865930

China, Natioal Health Commision of the People's Republic of China (2021). *Government report*. Retrieved from http://www.nhc.gov.cn/wjw/mtbd/202109/e2679465bae947daaacc1449972a6a93.shtml.

Corticos, N. D., & Duarte, C. C. (2021). COVID-19: The impact in US high-rise office buildings energy efficiency. *Energy and Buildings*, 249. https://doi.org/10.1016/j.enbuild.2021.111180

Coronavirus disease (COVID-19) outbreak situation. Retrieved from www.who.int/emergencies/diseases/novel-coronavirus-2019.

Ding, J. W., Yu, C. W., & Cao, S. J. (2020). HVAC systems for environmental control to minimize the COVID-19 infection. *Indoor And Built Environment, 29*(9), 1195–1201. https://doi.org/10.1177/1420326x20951968

Ding, J., & Cao, S.-J. (2021). Identification of zonal pollutant diffusion characteristics using dynamic mode decomposition: Towards the deployment of sensors. *Building And Environment*, 206. https://doi.org/10.1016/j.buildenv.2021.108379

Feng, Z. B., Cao, S. J., Wang, J. Q., Kumar, P., & Haghighat, F. (2021a). Indoor airborne disinfection with electrostatic disinfector (ESD): Numerical simulations of ESD performance and reduction of computing time. *Building And Environment*, 200. https://doi.org/10.1016/j.buildenv.2021.107956

Feng, Z., Cao, S. J., & Haghighat, F. (2021b). Removal of SARS-CoV-2 using UV+Filter in built environment. *Sustainable Cities and Society, 74*, Article 103226. https://doi.org/10.1016/j.scs.2021.103226

Gautam, K. R., Rong, L., Zhang, G. Q., & Abkar, M. (2019). Comparison of analysis methods for wind-driven cross ventilation through large openings. *Building and Environment, 154*, 375–388. https://doi.org/10.1016/j.buildenv.2019.02.009

Guo, M. Y., Xu, P., Xiao, T., He, R. K., Dai, M., & Miller, S. L. (2021). Review and comparison of HVAC operation guidelines in different countries during the COVID-19 pandemic. *Building and Environment*, 187. https://doi.org/10.1016/j.buildenv.2020.107368

Improving ventilation in your home. (2021). Retrieved from https://www.cdc.gov/coronavirus/2019-ncov/prevent-getting-sick/Improving-Ventilation-Home.html.

Leng, J. W., Wang, Q., & Liu, K. (2020). Sustainable design of courtyard environment: From the perspectives of airborne diseases control and human health. *Sustainable Cities and Society*, 62. https://doi.org/10.1016/j.scs.2020.102405

Li, X. T., Shen, C., & Yu, C. W. F. (2017). Building energy efficiency: Passive technology or active technology? *Indoor and Built Environment, 26*(6), 729–732. https://doi.org/10.1177/1420326x17719157

Liu, S. C., & Novoselac, A. (2015). Air Diffusion Performance Index (ADPI) of diffusers for heating mode. *Building and Environment, 87*, 215–223. https://doi.org/10.1016/j.buildenv.2015.01.021

Liu, X. P., Lv, X. X., Peng, Z., & Shi, C. L. (2020). Experimental study of airflow and pollutant dispersion in cross-ventilated multi-room buildings: Effects of source location and ventilation path. *Sustainable cities and society* (p. 52). https://doi.org/10.1016/j.scs.2019.101822

M.Gil-Baeza, J. Lizanae, Villanuevacd, J. A. B., M.Molina-Huelvaab, A. Serrano-Jimenezab, & Chacarteguicd, R. (2021). Natural ventilation in classrooms for healthy schools in the COVID era in Mediterranean climate. *Building and Environment*, 206. https://doi.org/10.1016/j.buildenv.2021.108345

Meng, M. R., Cao, S. J., Kumar, P., Tang, X., & Feng, Z. B. (2021). Spatial distribution characteristics of PM2.5 concentration around residential buildings in urban traffic-intensive areas: From the perspectives of health and safety. *Safety Science*, 141. https://doi.org/10.1016/j.ssci.2021.105318

Moey, L. K., Chan, K. L., Tai, V. C., Go, T. F., & Chong, P. L. (2021). Investigation on the effect of opening position across an isolated building for wind-driven cross ventilation. *Journal of Mechanical Engineering and Sciences, 15*(2), 8141–8152. https://doi.org/10.15282/jmes.15.2.2021.14.0639

Nikolopoulos, N., Nikolopoulos, A., Larsen, T. S., & Nikas, K. S. P. (2012). Experimental and numerical investigation of the tracer gas methodology in the case of a naturally cross-ventilated building. *Building and Environment, 56*, 379–388. https://doi.org/10.1016/j.buildenv.2012.04.006

Park, S., Choi, Y., Song, D., & Kim, E. K. (2021). Natural ventilation strategy and related issues to prevent coronavirus disease 2019 (COVID-19) airborne transmission in a school building. *Science of the Total Environment*, 789. https://doi.org/10.1016/j.scitotenv.2021.147764

Pei, G., Taylor, M., & Rim, D. (2021). Human exposure to respiratory aerosols in a ventilated room: Effects of ventilation condition, emission mode, and social distancing. *Sustainable Cities and Society*, 73. https://doi.org/10.1016/j.scs.2021.103090

Ren, C., Xi, C., Wang, J., Feng, Z., Nasiri, F., Cao, S. J., & Haghighat, F. (2021). Mitigating COVID-19 infection disease transmission in indoor environment using physical barriers. *Sustainable Cities and Society, 74*, Article 103175. https://doi.org/10.1016/j.scs.2021.103175

Riley, R. L., Riley, E. C., & Murphy, G. (1978). Airborne spread of measles in a suburban elementary-school. *American Review of Respiratory Disease, 117*(4), 255. -255.

Rothamer, D. A., Sanders, S., Reindl, D., & Bertram, T. H. (2021). Strategies to minimize SARS-CoV-2 transmission in classroom settings: Combined impacts of ventilation and mask effective filtration efficiency. *Science and Technology for the Built Environment, 27*(9), 1181–1203. https://doi.org/10.1080/23744731.2021.1944665

Rudnick, S. N., & Milton, D. K. (2003). Risk of indoor airborne infection transmission estimated from carbon dioxide concentration. *Indoor Air, 13*(3), 237–245. https://doi.org/10.1034/j.1600-0668.2003.00189.x

Sha, H., Zhang, X., & Qi, D. (2021). Optimal control of high-rise building mechanical ventilation system for achieving low risk of COVID-19 transmission and ventilative cooling. *Sustainable Cities and Society, 74*, Article 103256. https://doi.org/10.1016/j.scs.2021.103256

Shirzadi, M., Tominaga, Y., & Mirzaei, P. A. (2020). Experimental and steady-RANS CFD modelling of cross-ventilation in moderately-dense urban areas. *Sustainable Cities and Society*, 52. https://doi.org/10.1016/j.scs.2019.101849

Su, C. X., Lau, J., & Gibbs, S. G. (2016). Student absenteeism and the comparisons of two sampling procedures for culturable bioaerosol measurement in classrooms with and without upper room ultraviolet germicidal irradiation devices. *Indoor and Built Environment, 25*(3), 551–562. https://doi.org/10.1177/1420326x14562257

Tominaga, Y., Mochida, A., Yoshie, R., Kataoka, H., Nozu, T., Yoshikawa, M., & Shirasawa, T. (2008). AIJ guidelines for practical applications of CFD to pedestrian wind environment around buildings. *Journal of Wind Engineering and Industrial Aerodynamics, 96*(10-11), 1749–1761. https://doi.org/10.1016/j.jweia.2008.02.058

van Hooff, T., & Blocken, B. (2020). Mixing ventilation driven by two oppositely located supply jets with a time-periodic supply velocity: A numerical analysis using computational fluid dynamics. *Indoor and Built Environment, 29*(4), 603–620. https://doi.org/10.1177/1420326x19884667

van Hooff, T., Blocken, B., & Tominaga, Y. (2017). On the accuracy of CFD simulations of cross-ventilation flows for a generic isolated building: Comparison of RANS, LES and experiments. *Building and Environment, 114*, 148–165. https://doi.org/10.1016/j.buildenv.2016.12.019

van Moeseke, G., Gratia, E., Reiter, S., & De Herde, A. (2005). Wind pressure distribution influence on natural ventilation for different incidences and environment densities. *Energy and Buildings, 37*(8), 878–889. https://doi.org/10.1016/j.enbuild.2004.11.009

Wang, J. Q., Huang, J. J., Feng, Z. B., Cao, S. J., & Haghighat, F. (2021). Occupant-density-detection based energy efficient ventilation system: Prevention of infection transmission. *Energy and Buildings*, 240. https://doi.org/10.1016/j.enbuild.2021.110883

Wu, C. L., Wang, H. W., Cai, W. J., He, H. D., Ni, A. N., & Peng, Z. R. (2021). Impact of the COVID-19 lockdown on roadside traffic-related air pollution in Shanghai, China. *Building and Environment*, 194. https://doi.org/10.1016/j.buildenv.2021.107718

Wu, Y., & Niu, J. L. (2016). Assessment of mechanical exhaust in preventing vertical cross household infections associated with single-sided ventilation. *Building And Environment, 105*, 307–316. https://doi.org/10.1016/j.buildenv.2016.06.005

Xi, C., Ren, C., Wang, J., Feng, Z., & Cao, S.-J. (2021). Impacts of urban-scale building height diversity on urban climates: A case study of Nanjing, China. *Energy And Buildings*, 251. https://doi.org/10.1016/j.enbuild.2021.111350

Xu, C. W., Luo, X. L., Yu, C., & Cao, S. J. (2020). The 2019-nCoV epidemic control strategies and future challenges of building healthy smart cities. *Indoor and Built Environment, 29*(5), 639–644. https://doi.org/10.1177/1420326x20910408

Zheng, K., Ortner, P., Lim, Y. W., & Zhi, T. J. (2021). Ventilation in worker dormitories and its impact on the spread of respiratory droplets. *Sustainable Cities and Society, 75*, Article 103327. https://doi.org/10.1016/j.scs.2021.103327

Zhu, H. C., Ren, C., & Cao, S. J. (2021). Fast prediction for multi-parameters (concentration, temperature and humidity) of indoor environment towards the online control of HVAC system. *Building Simulation, 14*(3), 649–665. https://doi.org/10.1007/s12273-020-0709-z

Zivelonghi, A., & Lai, M. (2021). Mitigating aerosol infection risk in school buildings: The role of natural ventilation, volume, occupancy and CO2 monitoring. *Building and Environment*, 204. https://doi.org/10.1016/j.buildenv.2021.108139